Accepted Manuscript

Title: A structural basis for the amphiphilic character of alginates – Implications for membrane fouling

Authors: Matthew B. Stewart, Darli T. Myat, Michael Kuiper, Richard J. Manning, Stephen R. Gray, John D. Orbell

Please cite this article as: Stewart, Matthew B., Myat, Darli T., Kuiper, Michael., Manning, Richard J., Gray, Stephen R., & Orbell, John D., A structural basis for the amphiphilic character of alginates – Implications for membrane fouling.*Carbohydrate Polymers* http://dx.doi.org/10.1016/j.carbpol.2017.01.072

A structural basis for the amphiphilic character of alginates – implications for membrane fouling

Matthew B. Stewart[a,b] , Darli T. Myat[a,b], Michael Kuiper[c], Richard J. Manning[a,b], Stephen R. Gray[a,b] and John D. Orbell[a,b*]

[a]*Institute for Sustainability and Innovation (ISI), Victoria University, PO Box 14428, Melbourne, VIC 8001, Australia*

[b]*College of Engineering and Science, Victoria University, PO Box 14428, Melbourne, VIC 8001, Australia*

[c]*Victorian Life Sciences Computation Initiative, the University of Melbourne, Parkville Campus, 187 Grattan Street, Carlton, VIC 3010, Australia*

Corresponding author at: Institute for Sustainability and Innovation (ISI), College of Engineering and Science, Victoria University, PO Box 14428, Melbourne, VIC 8001, Australia. Tel: +61 3 9919 8066.

E-mail addresses: Matthew.Stewart@vu.edu.au (M.B. Stewart), mkuiper@unimelb.edu.au (M.Kuiper), John.Orbell@vu.edu.au (J.D. Orbell), Stephen.Gray@vu.edu.au (S.R. Gray)

Highlights

- Alginates with high M content foul (bind to) hydrophobic membranes at low and neutral pH.
- M has been shown by quantum chemical calculations to be to be uniquely amphiphilic.
- A hydrophobic patch on M allows alginate polymers containing M to bind to a hydrophobic surface.
- The mechanism of alginate binding to a hydrophobic membrane (polypropylene) has been demonstrated by MD simulations.
- The hydrophobic patch of M is essential for the functioning of the enzyme mannuronan C-5 epimerase AlgE4.

Abstract

Ostensibly hydrophilic alginates are known to foul hydrophobic membranes, under various conditions. Here, controlled experiments have been conducted at high and low pH on the fouling of a polypropylene membrane by alginate and the results suggest that the observed fouling is due to an intrinsic property of the alginate. Thus quantum chemical calculations on the M and G monomers of alginate reveal that M adopts an equilibrium geometry that is hydrophilic on one face and hydrophobic on the other, i.e. is potentially amphiphilic. Molecular dynamics simulations on short alginate chains of different sequences interacting with a modelled polypropylene surface, show that this characteristic is carried over to the polymer and results in hydrophobic patches along the chain that facilitate attractive interactions with the polypropylene surface. This concept is buttressed by an analysis of the binding characteristics of a previously reported X-ray structure of the mannuronan C-5 epimerase AlgE4 enzyme.

1. Introduction

Membrane-based separation technologies are widely utilised, with broad applications including desalination, water reclamation and desalination - as well as in the food and dairy processing industries (Daufin, Excudier, Carrère, Bérot, Fillaudeau & Decloux, 2001; Lee, Arnot & Mattia, 2011; Pouliot, 2008; Wintgens et al., 2005). A major issue for all such applications is the challenge of organic fouling (Lee, Amy & Croué, 2004). This is particularly difficult for the reclamation and treatment of natural surface waters, where the composition and concentration of natural organic matter (NOM), as well as other solutes such as metal ions, can be constantly fluctuating. Due to the highly complex and variable nature of

NOM in bulk water samples, researchers often select model compounds that represent a particular category. For example, bovine serum albumin (BSA) may be employed to represent proteins and sodium alginate may be used to represent the high molecular weight hydrophilic biopolymer fraction. Thus their individual and synergistic effects on membrane behaviour may be scrutinized (Gray, Dow, Orbell, Tran & Bolto, 2011; Gray et al., 2008; Henderson et al., 2011; Jermann, Pronk, Meylan & Boller, 2007; Myat, Stewart, Mergen, Zhao, Orbell & Gray, 2014).

Sodium alginate is the sodium salt of alginic acid, which is a linear polyuronic acid produced naturally by brown algae and some bacteria (Donati & Paoletti, 2009; Gorin & Spencer, 1966; Goven, Fyfe & Jarman, 1981). Alginates are unbranched copolymers produced from irregular, but generally not random, blocks of two monomers; namely β-D-mannuronic acid (M) and α-L-guluronic acid (G). In alginate, these two monomers are linked *via* $(1 \rightarrow 4)$ glycosidic bonds, to form three distinct types of sequence blocks – homopolymeric blocks of both M and G, as well as the heteropolymeric block of alternating G and M subunits. A schematic diagram of such polymer sequences is depicted in Fig 1.

In spite of such polysaccharides being regarded as ostensibly hydrophilic in nature, due to the preponderance of hydrogen bonding functional groups such as hydroxyl and carboxylate, recent studies that have examined the effects of sodium alginate on membrane fouling have found that alginates adhere to both hydrophilic (Katsoufidou, Yiantsios & Karabelas, 2007, 2008; Nghiem & Espendiller, 2014) and hydrophobic (Gray, Dow, Orbell, Tran & Bolto, 2011; Guo, Chen & Hu, 2009; Less, Ang & Elimelech, 2006) polymeric membrane surfaces, such as polyamide and polypropylene, respectively. Thus whilst there is research at the molecular level on how alginate interacts and irreversibly binds to hydrophilic membrane surfaces, including directly *via* metal ion bridging (Xiang, Liu, Mi & Leng, 2013) or

hydrogen bonding (Xiang, Liu, Mi & Leng, 2014), there is a paucity of such information as to how the supposedly hydrophilic alginate chains, counterintuitively perhaps, bind in a seemingly thermodynamically unfavourable way to hydrophobic surfaces. To date, there has been no molecular-scale explanation offered for this phenomenon.

The work presented here addresses this problem by identifying the origin of the amphiphilic nature of alginates through quantum chemical characterization of the individual M and G monomers and subsequent molecular dynamics simulations that simulate actual interactions between alginate chains and a model hydrophobic polypropylene surface. These studies have also been benchmarked to complimentary laboratory membrane fouling experiments and compared to a biochemical example of hydrophobic enzymatic active site interacting with its alginate derivative substrate.

2. Experimental Method

2.1 Feed solution preparation

Sodium alginate from brown algae was obtained from Sigma-Aldrich, with the molecular weight specified by the manufacturer as being in the range of 12-80 kDa and a composition of 39% G and 61% M. A stock solution containing 1g/L of sodium alginate in DI water was prepared.

2.2 Membranes

A single hollow fibre (HF) membrane filtration rig was used to examine the fouling rate of an sodium alginate feed solution. A single fibre polypropylene membrane obtained from Memcor with an outside diameter of 0.50 mm, an inside diameter of 0.25 mm and 600 mm in length, was inserted into a transparent polyurethane tubing and then sealed with epoxy resin. This membrane material is hydrophobic polypropylene with a nominal pore size of 0.2 μm as specified by the membrane supplier. The filtration experiments were performed at constant

flux and the water was pumped from the outside to the inside of the hollow fibre. The filtrate was weighed on a balance and liquid backwashing of the membrane was achieved via pressurized water and a series of valves. The backwashing regime consisted of a flow reversal for 20s so that filtered water entered the inside of the hollow fibre and forced out any accumulated foulant to the outside. The outside of the fibre was then flushed by a cross flow of feed water past the membrane for a further 20 s. A data acquisition system was used to control the backwash sequence as well to record the transmembrane pressure (TMP) via a pressure transducer. The ambient air temperature was also recorded during the run. Clean water fluxes were also monitored before each test.

2.3 Membrane filtration

The filtration unit was operated with pumped permeate (controlled flux) and a dead-end configuration. The feed solution was supplied to the outside of the HF membrane module using a positive displacement pump at a set flow rate, and the filtrate (permeate) was collected from the inside of HF membrane. The TMP was recorded continuously and backwashing with clean water was carried out for 5 minutes after every hourly filtration cycle.

2.4 Quantum chemical calculations

Equilibrium geometries and electrostatic potential energy maps for the alginate monomers G and M and their respective anions were computed at the B3LYP/6-31+G* level of theory SPARTAN06 (Wavefunction, Inc.)

2.4 Molecular dynamics

All simulations were carried out using a modified CHARMM all22 force field (MacKerell et al., 1998) and the NAMD 2.7 package (Phillips et al., 2005). Topology and parameter files for carbohydrates were appropriately edited to allow for the addition of the carboxylic acid groups to the parameterised carbohydrates. Atomic point charges were recalculated from density functional equilibrium geometry calculations - at the B3LYP/6-31G(d) level of theory on the G and M monomers and applied to the polymer topology. Initially, fully deprotonated hexamers of sequence GGMMGG were constructed using the Visual Molecular Dynamics (VMD) program (Humphrey, Dalke & Schulten, 1996) and optimised using MD in a TIP3P water box which measured 50 Å x 50 Å x 50 Å, which included six sodium ions to neutralise the charge of the hexamer. These optimisations involved 1000 conjugate gradient minimization steps, followed by 2 ns of molecular dynamics simulation time under NPT conditions in a periodic box. The temperature and pressure was maintained using Langevin dynamics as implemented in NAMD. This optimised hexamer was used as the starting geometry for the polypropylene membrane simulations. The deprotonated decamers were similarly optimised as previously described for the deca-G (Stewart, Gray, Vasiljevic & Orbell, 2014a), deca-M and penta-GM (Stewart, Gray, Vasiljevic & Orbell, 2014b) chains.

In order to study how these, now-optimized, hexamer and decamers chains interact with a polypropylene membrane, a model of this surface was also required. Again, atomic point charges were calculated from density functional equilibrium geometry calculations, at the B3LYP/6-31G(d) level of theory. The surface was developed by building linear chains of polypropylene that were 12 monomers long. Fifteen of these chains were then placed approximately 3.5 Å apart relative in two rows, with the top row lining up with the space between the lower chains. This construct was solvated in a TIP3P waterbox 70 Å x 70 Å x70 Å in size, and subjected to MD simulations in order to form a consolidated polymer mass. This MD simulation consisted of 1000 conjugate gradient minimization steps, followed by 2

ns of molecular dynamics simulation time under NPT conditions in a periodic box. This produced a polymer model that consisted of crystalline and amorphous sections, similar to a real ultrafiltration membrane surface.

Finally, simulations were carried out that utilized the optimised alginate models. These simulations consisted of both the hexamer as well as the three individual decamer sequences interacting with the polypropylene model. Specifically, one simulation was constructed which consisted of six GGMMGG hexamer chains that were initially placed greater than 12 Å away from the surface of the polypropylene model, so as to not artificially bias the simulation towards alginate-surface interactions, before being solvated and neutralising sodium atoms being added. All atoms of the polypropylene model were frozen, due to the fact that the model, in order to contain varying surface characteristics in a cylindrical shape, was in a non-equilibrium state. When not frozen, the polypropylene model assumed an amorphous, spherical shape, which is unlike the membrane surface being modelled in this work. This simulation was carried out under identical conditions to those described above for the optimization of the hexamer, albeit within a larger waterbox, measuring 81 Å x 81 Å x 81 Å.

The simulations containing the decamer sequences differed from the initial simulation, as nine chains were used, again placed greater than 12 Å away from the surface. This construct was also solvated and ions were added to neutralise the charges of the alginate chains. The waterbox sizes varied depending upon sequence, with a 20 Å buffer in all three axes added to ensure no periodic effects. The simulations were then carried out under a simulated annealing regime, as in previous work (Stewart, Gray, Vasiljevic & Orbell, 2014a, b; Hecht & Srebnik, 2016). Again, the polypropylene model atoms were frozen.

3. Results and discussion

In order to provide insights into the phenomenon of ostensibly 'hydrophilic' alginate polymer chains interacting with hydrophobic polypropylene surfaces such as polypropylene, comprehensive and systemic experimental and computational studies were initiated, *vide supra*. The complementary experimental *and* theoretical design of this research ensures that the insights and outcomes have potential 'real-world' relevance – not only in the area of organic membrane fouling, but potentially in other fields that utilise the chemistry of alginates. Thus the theoretical work presented here has been designed to complement the membrane fouling experimental data and to provide an insight into the phenomenon of 'hydrophilic' alginate chains interacting strongly with hydrophobic polymer surfaces resulting in irreversible fouling.

3.1 Membrane filtration experiments

In order to standardise the response of alginate to the polypropylene surface – in both acidic and neutral environments – specific experiments were carried out to collect this data. The results of these experiments, Fig. 2, reveal that the alginate in the acidic solution (pH = 3) fouled the polypropylene membrane quicker, and more severely, than for the higher (near neutral) pH = 6 solution, although notably fouling occurs in *both* cases. No precipitation was observed in the alginate solutions themselves, either at pH 3 or pH 6.

In membrane fouling studies that incorporate a backwash process, such as those described here, if the foulant-foulant interactions are similar (the same chemistry), then the relative adhesion of the foulant to a membrane surface can be determined by the backwash efficiency. Indeed, a previous publication by the authors (Gray, Dow, Orbell, Tran & Bolto, 2011) has shown that alginate is easily backwashed from a hydrophilic PVDF membrane (a hydrophilic PVDF membrane is likely to have the surface active additive PVP - a hydrophilic brush

polymer - on the surface). Hence, the dramatically reduced backwashing efficiency observed in the current results, with a polypropylene membrane, reflects a greater strength of adhesion between the membrane and fouling layer (in this case the polypropylene membrane and alginate). The constant fouling of the membrane and low backwashing efficiency of the membrane as depicted in Fig. 2, compared to the previously published hydrophilic PVDF membrane, that showed no continual fouling increase over time, clearly indicates adhesion between the membrane (polypropylene) and the fouling layer (alginate).

Thus the fouling is less reversible at the lower pH, suggesting that the protonated alginate is more attracted to the polypropylene surface than the deprotonated alginate. This also suggests that the mechanism of interaction between the alginate and the polypropylene surface is not ion-mediated (i.e. *via* carboxylate-metal ion bridging between alginate and oxygen-containing groups on the polypropylene surface), nor due solely to colloidal filtering blocking the pores of the membrane (as such macromolecular constructs would be largely removed with backwashing). Rather, the suggestion is that such fouling is related to an intrinsic property of the alginate itself. Therefore, theoretical studies were deemed to be of value to determine what mechanisms are at play. In this regard, systematic computational modelling investigations were carried out in order to characterise the potential interactions of alginate with a hydrophobic polypropylene surface, starting with a detailed examination of the monomers themselves.

 3.2 The alginate monomers

An initial study of the structural and electronic characteristics of the protonated and deprotonated monomers, G and M, was carried out with a view to qualitatively assessing their equilibrium structures together with their potential hydrophobic and hydrophilic characteristics. Thus the computed equilibrium geometries of these molecules are depicted in

Fig. 3. Notably, *both the protonated and anionic forms* of the M monomer display a structurally and electronically segregated character, Fig. 3 (a) and (b) respectively. Thus one side (face) of both molecules is potentially hydrophobic and the other side (face) is potentially hydrophilic, as evidenced by the isolation of four non-polar hydrogen atoms on one face and the oxygen containing moieties on the other. The protonated and anionic forms of the G monomer do not show such segregation, Fig. 3 (c) and (d). Thus this attribute is unique to the M monomer and immediately suggests an *inherent* structural basis for the existence of a hydrophobic region, or "patch", on M that could be carried over, and even enhanced or extended, in polymers that incorporate this monomer. The computed electrostatic potential energy surfaces of both faces of the M monomer are shown in Fig. 4 and highlight this "hydrophobic patch". On the other hand, the G monomer displays a surface whereby the electrostatic potential over the molecular surface suggests an even distribution of hydrophilic character with no obvious segregation. The presence of this patch on M, especially if conserved or enhanced in the polymer, could impart the amphiphilicity that is evident in alginate. Notably, molecules usually considered to be amphiphilic derive this characteristic *longitudinally* (e.g. surfactants or vitamin E - with a polar 'head' and a non-polar 'tail') rather than *laterally* across a molecule, as is observed here with the M monomer. Having uncovered this fundamental attribute of the M monomer, our investigations were broadened to determine if this hydrophobic patch was indeed conserved and possibly enhanced in alginate chains with M content and repeating M sequences.

3.3 Oligomers

Following the characterization of the of the amphiphilic character of the M monomer, *vide supra*, the next step was to investigate whether the potential hydrophobic patch exists and is

accessible in alginate polymers. In order to probe this, firstly, a hypothetical hexamer strand was built of sequence GGMMGG to assess the potential amphiphilicity arising from two adjacent M monomers in an oligomer. These hexamer chains were then utilised in a short MD simulation in the presence of an idealized polypropylene surface (surface oxidation was not accounted for) and neutralising ions (for details and method, see Section 2 above). This short simulation was initially designed to be a rapid 'proof of concept' experiment to define any interactions between the theoretical alginate oligomer and the polypropylene surface. This simulation also allowed for the validation of the modified force field parameters that were developed in-house, specifically regarding the stereochemistry of the bound monomers and the general behaviour of the alginate model. The result of this simulation showed that there was indeed an explicit area of interaction between the MM section of the hexamer with the modelled polypropylene surface, in which water was excluded from the interface of these two surfaces, suggestive of a hydrophobic interaction, Fig. 5.

Whilst this simulation provides evidence that alginates, via the M residue(s), may bind to a hydrophobic surface, it is acknowledged that this particular sequence is unlikely to occur in native alginates. Upon further analysis of this simulation, it was noticed that these hexamers possesed an unrealistically low barrier of rotation around the MM 1,4-glycosidic linkage, which resulted in hexamer chains that were in a *cis* conformation with respect to their hydrophobic patches, rather than the native *trans* orientation that would be generally expected in nature, due to the repulsion of the anionic carboxylate groups (DeRamos, Irwin, Nauss & Stout, 1997; Perry IV, Cygan & Mitchell, 2006). However, recent work has shown that such a *cis* orientation can theoretically occur under the influence of coordinating Ca^{2+} ions (Stewart, Gray, Vasiljevic & Orbell, 2014a) although, in this simulation, only sodium

was present to balance the charges - and this conformation could also be stabilized by an energetically favorable interaction with the polypropylene surface. For the subsequent calculations on actual known sequences the appropriate torsion parameters were modified to yield more realistic rotational barriers. Therefore, these investigations were broadened to incorporate all three known sequences for native alginates, namely: homopolymeric G (poly-G), homopolymeric M (poly-M) and alternating heteropolymeric GM (poly-GM) decamers that, gratifyingly, provide clear evidence of similar hydrophobic interactions with the modelled polypropylene surface. These are also depicted graphically and described in more detail in Myat, 2013.

3.4 Decamers – poly-G, poly-M and poly-GM

Upon construction and initial energy minimisation of these polymeric decamer chains, it appeared that all three sequences display some hydrophobic potential, in so far as there were clearly defined regions on these decamer chains that are rich in adjacent non-polar hydrogen atoms. As can be seen from space filling models of these chains as computed from MD optimized geometries, Fig. 6, even the poly-G chains display a 'ribbon' of non-polar hydrogen atoms which runs the length of the chain, and the poly-M and poly-GM chains contain localised hydrophobic 'patches' based around the M monomer. Also of note, is that the patches identified in the M-containing sequences are slightly different from each other, with the poly-GM sequences recruiting hydrogen atoms from the neighbouring G monomers, representing a potential enhancement of this effect in the heteropolymeric sequence.

Each of these decamer sequences were also investigated independently *via* molecular dynamics simulations, in the presence of a polypropylene surface, and under two representative pH conditions – namely pH < 2 and pH > 6. The pH conditions were represented in the simulations by constructing the alginate chains as either fully protonated (low pH) or fully deprotonated (neutral and above pH). These simulations also contained sodium ions at a similar concentration to those used in the complementary experimental procedure. The MD simulations were then analysed in detail, and the van der Waals interaction energies of the alginate chains interacting with the polypropylene surface were also extracted from the MD trajectories utilising the tools within VMD (Humphrey, Dalke & Schulten, 1996). The van der Waals energy of the two interacting species were used as the measure of this interaction energy, as the electrostatic interaction was negligible due to the low point charges assigned to the polypropylene atoms. Furthermore, these energies were extracted from the final 200ps of simulation time – which corresponds to temperatures of approximately 300K – to ensure that the simulation outcomes are indicative of the room temperature experiments described in Section 3.1.

When the van der Waals interaction energies are compared for each of the three simulations at neutral or above pH, there is a clear preference of deca-M (-7.489 kcal/mol) interacting with the polypropylene surface, followed by penta-GM (-3.681 kcal/mol) and deca-G (-2.417 kcal/mol). This preference is as expected in the light of the existence of a hydrophobic patch on the M monomer. With respect to the low pH simulation trajectories, for all three sequences, there are many more chains that are observed interacting with the polypropylene surfaces compared to the higher pH simulation. This, together with the higher van der Waals interaction energies for these protonated sequences, Table 1, is also not unexpected and nicely reflects the enhanced fouling profile at low pH as observed in the complementary membrane fouling experiments, Fig.2. Furthermore, these outcomes demonstrate that the

interaction of alginates with a hydrophobic polypropylene surface is *not dependent* on metal ion coordination, as the protonated alginate chains do not have an ionic binding site available, due to the carboxyl groups being protonated. This provides evidence that the hydrophobic interactions at the core of such alginate-polypropylene interactions are an inherent property of the alginates themselves, especially but not exclusively, at low pH values.

From Table 1, it may be seen that at low pH, the sequences containing the M monomer interact significantly with the polypropylene surface. From the perspective of the numbers of chains interacting with the polypropylene surface, the penta-GM chains were the most effective, with nine of the ten chains present in this simulation interacting with the surface. This was closely followed by the deca-M sequence, with seven out of ten chains showing attraction to the polypropylene surface. The non-M monomer-containing sequence, deca-G, showed only three out of ten chains interacting with the surface. Therefore, if the sum of the average interaction energies of each interacting chain within these systems is considered, then it appears that penta-GM has the highest attraction to the surface, followed by deca-M, with the deca-G sequence again showing the least total interaction energy. This order is similar to that evidenced in the neutral pH simulations – with the M monomer-containing sequences being most attracted to the polypropylene surface *via* hydrophobic patches; albeit in these simulations it is the penta-GM system that shows the greater attraction, rather than the deca-M. This is reflected in the average interaction energy for these systems, with each interacting penta-GM chain experiencing -14.917 kcal/mol of van der Waals attraction, compared to -13.952 kcal/mol for the deca-M system, and can be attributed to the hydrophobic patch of M recruiting one or more hydrogen atoms in a neighbouring G, Fig. 6.

The importance of the ampihilic character of the M monomer, arising from its identified unique geometry and subsequent hydrophobic patch, is evident from the above investigations

for both pH environments, leading to enhanced attractive van der Waals interaction energies with the polypropylene surface.

It is important to stress the successful benchmarking of the computational investigations with the complementary membrane fouling experiments, given that the alginate used (as obtained from Sigma-Aldrich – see methods section) in the latter experiments has a composition of 39% G and 61% M. Therefore, it is not unexpected that an alginate with such a high relative amount of the M monomer is an significant foulant of the hydrophobic membrane, especially at acidic pH values.

3.5 Further evidence

The findings emanating from the discovery of the hydrophobic patch of M, as presented in this paper, are buttressed by research that highlights the significance and the potential evolutionary conservation of such a structural/electronic feature. This relates to the published X-ray crystal structure of the enzyme mannuronan C-5 epimerase AlgE4 (Rozeboom et al., 2008)[1] . This enzyme is involved in the production of alginates, in so far as it converts some of the M subunits in the poly-M chains that are produced by a particular organism, into G subunits. The aspect of this X-ray crystal structure that highlights the importance of the hydrophobic patch of M is the fact that, in the crystal structure, the enzyme is complexed with a mannuronon trisaccharide substrate in the active site. Upon close examination of this substrate within the active site, Fig. 7, there is a leucine residue (Leu-228) in a flexible loop that appears to hold the ligand in place, as well as a valine residue (Val-201) in the β-sheet that interacts with an adjacent M subunit. Specifically, this leucine residue, *via* its isobutyl side-chain, interacts partially with an exposed hydrophobic patch on the central M monomer

---

[1] PDB ID: 2PYH, as lodged with the Research Collaboratory for Structural Bioinformatics Protein Databank (RCSB PDB) (Berman et al., 2000)

of the bound ligand and the valine residue interacts with a second hydrophobic patch *via* its isopropyl side chain. This intriguing observation provides further evidence of the importance of the intrinsic hydrophobic patch of M that allows it to attractively interact with other hydrophobic regions and surfaces. Therefore, in terms of membrane fouling, alginates interact with hydrophobic surfaces by essentially 'hijacking' a binding interaction motif that is essential to the biological production of the alginates themselves, and is thus an inherent property of these biopolymers.

4. Conclusions

This work has explored the phenomenon of apparently 'hydrophilic' alginate polymer chains forming attractive interactions with 'hydrophobic' membrane surfaces, leading to irreversible fouling of membranes with such surface characteristics. Experimentally, this study applied sodium alginate solutions at two different pH values, to examine the fouling rates for a polypropylene hollow-fibre membrane. The low pH alginate solution rapidly and irreversibly fouled the membrane, compared to the neutral pH solution, which still fouled the membrane, albeit at a less rapid pace.

Complementary computational chemistry investigations were employed to provide insights into possible molecular-scale interactions that might be responsible for the apparent attraction between alginates and the polypropylene surface. Initially, these studies examined both G and M monomers for any intrinsic characteristics that might contribute to an amphiphilic character in the polymer and established that the M monomer was uniquely asymmetric in terms of presenting segregated hydrophilic and hydrophobic faces on opposing surfaces of the molecule, both in the neutral and anionic forms. The hydrophobic face was duly termed the M "hydrophobic patch". Molecular dynamics simulations, that include calculated interaction energies, were then carried out at low and near neutral pHs and these confirmed

16

that the M hydrophobic patch does indeed contribute to the binding of the different alginate sequences to a model polypropylene surface. These studies highlight the persistence of the unique molecular structure of the M monomer. The robustness of this structural motif is evidenced by the existence of extended hydrophobic patches in the polymers, includingthe recruitment of adjacent non-polar hydrogens as seen in the alternating penta-GM sequence. These computational studies were found to be entirely consistent with the concomitant benchmarking membrane fouling experiments.

Further evidence supporting the presence, and hydrophobic activity, of the M patch is provided from the previously published X-ray crystal structure of the mannuronan C-5 epimerase AlgE4 enzyme, which was crystallized with a mannuronon trisaccharide substrate molecule. This structure also shows two hydrophobic binding interactions involving the M hydrophobic patch identified in our simulations. Therefore, not only have alginates been shown here to possess intrinsic amphiphilic character, but such interactions are evolutionarily conserved by the very enzyme that is involved in producing these biopolymers. Certainly, this amphiphilic character of alginates, as delineated here, should be taken into account when designing membrane treatment options for waters high in alginate content, irrespective of the ionic environment.

5. Acknowledgments

References

Berman, H. M., Westbrook, J., Feng, Z., Gilliland, G., Bhat, T. N., Weissig, H., Shindyalov, I. N., & Bourne, P. E. (2000). The Protein Data Bank. *Nucleic Acids Research, 28*, 235-242.

Daufin, G., Excudier, J.-P., Carrère, H., Bérot, S., Fillaudeau, L., & Decloux, M. (2001). Recent and Emerging Application of Membrane Processes in the Food and Dairy Industry. *Food and Bioproducts Processing, 79*(2), 89-102.

DeRamos, C. M., Irwin, A. E., Nauss, J. L., Stout, B. E. (1997). 13CNMR and molecular modeling studies of alginic acid binding with alkaline earth and lanthanide metal ions. *Inorganica Chimica Acta*, 256, 69-75.

Donati, I., & Paoletti, S. (2009). Material Properties of Alginates. In B. H. A. Rehm (Ed.). *Alginates: Biology and Applications*: Springer Berlin Heidelberg.

Gorin, P. A. J., & Spencer, J. F. T. (1966). Exocellular alginic acid from *Azotobacter Vinelandii*. *Canadian Journal of Chemistry, 44*, 993-998.

Goven, J. R., Fyfe, J. A., & Jarman, T. R. (1981). Isolation of alginate-producing mutants of *Pseudomonas fluorescens*, *Pseudomonas putida* and *Psuedomonas mendocina*. *Journal of General Microbiology, 125*, 217-220.

Gray, S. R., Dow, N., Orbell, J. D., Tran, T., & Bolto, B. A. (2011). The significance of interactions between organic compounds on low pressure membrane fouling. *Water Science and Technology, 64*(3), 632-639.

Gray, S. R., Ritchie, C. B., Tran, T., Bolto, B. A., Greenwood, P., Busetti, F., & Allpike, B. (2008). Effect of membrane character and solution chemistry on microfiltration performance *Water Research, 42*(3), 743-753.

Guo, X., Chen, X., & Hu, W. (2009). Studies on cleaning the polyvinylchloride ultrafiltration membrane fouled by sodium alginate. *Environmental Technology, 30*(5), 431-435.

Haug, A., Larsen, B., & Smidsrød, O. (1966). A study on the constitution of alginic acid by partial hydrolysis. *Acta Chemica Scandinavica, 20*, 183-190.

Haug, A., Larsen, B., & Smidsrød, O. (1967). Studies on the sequence of uronic acid residues in alginic acid. *Acta Chemica Scandinavica, 21*, 691-704.

Haug, A., & Smidsrød, O. (1965). Fractionation of alginate by precipitation with calcium and magnesium ions. *Acta Chemica Scandinavica, 19*, 1221-1226.

Hecht, H & Srebnik, S. (2016). Structural characterization of sodium alginate and calcium alginate. *Biomacromolecules, 17*, 2160-2167.

Henderson, R. K., Subhi, N., Antony, A., Khan, S. J., Murphy, K. R., Leslie, G. L., Chen, V., Stuetz, R. M., & Le-Clech, P. (2011). Evaluation of effluent organic matter fouling in ultrafiltration treatment using advanced organic characterisation techniques. *Journal of Membrane Science, 382*, 50-59.

Humphrey, W., Dalke, A., & Schulten, K. (1996). VMD - Visual Molecular Dynamics. *Journal of Molecular Graphics, 14*, 33-38.

Jermann, D., Pronk, W., Meylan, S., & Boller, M. (2007). Interplay of different NOM fouling mechanisms during ultrafiltration for drinking water production. *Water Research, 41*(8), 1713-1722.

Katsoufidou, K., Yiantsios, S. G., & Karabelas, A. J. (2007). Experimental study of ultrafiltration membrane fouling bu sodium alginate and flux recovery by backwashing. *Journal of Membrane Science, 300*, 137-146.

Katsoufidou, K., Yiantsios, S. G., & Karabelas, A. J. (2008). An experimental study of UF membrane fouling by humic acid and sodium alginate solutions: the effect of backwashing on flux recovery. *Desalination, 220*, 214-227.

Lee, K. P., Arnot, T. C., & Mattia, D. (2011). A review of reverse osmosis membrane materials for desalination - Development to date and future potential. *Journal of Membrane Science, 370*(1-2).

Lee, N. H., Amy, G., & Croué, J. P. (2004). Identification and understanding of fouling in low presure membrane (MF/UF) filtration by natural organic matter (NOM) *Water Research, 38*(20), 4511-4523.

Less, S., Ang, W. S., & Elimelech, M. (2006). Fouling of reverse osmosis membrane by hydrophilic organic matter: implications for water reuse. *Desalination, 187*(1-3), 313-321.

MacKerell, A. D., Bashford, D., Bellott, M., Dunbrack, R. L., Evanseck, J. D., Field, M. J., Fischer, S., Gao, J., Guo, H., Ha, S., Joseph-McCarthy, D., Kuchnir, L., Kuczera, K., Lau, F. T. K., Mattos, C., Michnick, S., Ngo, T., Nguyen, D. T., Prodhom, B., Reiher, W. E., Roux, B., Schlenkrich, M., Smith, J. C., Stote, R., Straub, J., Watanabe, M., Wiórkiewicz-Kuczera, J., Yin, D., & Karplus, M. (1998). All-Atom Empirical Potential for Molecular Modeling and Dynamics Studies of Proteins. *The Journal of Physical Chemistry B, 102*(18), 3586-3616.

Myat, D. T., Stewart, M. B., Mergen, M., Zhao, O., Orbell, J. D., & Gray, S. R. (2014). Experimental and computational investigations of the interactions between model organic compounds and subsequent membrane fouling. *Water Research, 28*, 108-118.

Myat, D.T. (2013). Experimantal and theoretical investigations of membrane fouling - examining the nature of foulant-foulant and foulant-mambrane interactions. PhD thesis, Victoria University, Melbourne, Australia.

Nghiem, L. D., & Espendiller, C. (2014). Effects of organic and colloidal fouling on the rejection of two pharmaceutically active compounds (PhACs) by nanofiltration processes: role of membrane foulants. *Desalination and Water Treatment, 52*(4-6), 633-642.

Perry IV, T. D., Cygan, R. T., Mitchell, R. (2006). Molecular models of alginic acid: Interactions with calcium ions and calcite surfaces. *Geochimica et Cosmochimica Acta,* 70, 3508-3532.

Phillips, J. C., Braun, R., Wang, W., Gumbart, J., Tajkhorshid, E., Villa, E., Chipot, C., Skeel, R. D., Kale, L., & Schulten, K. (2005). Scalable molecular dynamics with NAMD. *Journal of Computational Chemistry, 26*, 1781-1802.

Pouliot, Y. (2008). Membrane processes in dairy technology - From a simple idea to worldwide panacea. *International Dairy Journal, 18*(7), 735-740.

Rozeboom, H. J., Bjerkan, T. M., Kalk, K. H., Ertesvag, H., Holtan, S., Aachmann, F. L., Valla, S., & Dijkstra, B. W. (2008). Structural and mutational characterization of the catalytic A-module of the mannuronan C-5-epimerase AlgE4 from Aztobacter vinelandii. *Journal of Biological Chemistry, 283*, 23819-23828.

Stewart, M. B., Gray, S. R., Vasiljevic, T., & Orbell, J. D. (2014a). Exploring the molecular basis for the metal-mediated assembly of alginate gels. *Carbohydrate Polymers, 102*, 246-253.

Stewart, M. B., Gray, S. R., Vasiljevic, T., & Orbell, J. D. (2014b). The role of poly-M and poly-GM sequences in the metal-mediated assembly of alginate gels. *Carbohydrate Polymers, 112*, 486-493.

Wintgens, T., Melin, T., Schäfer, A., Khan, S., Muston, M., Bixio, D., & Thoeye, C. (2005). The role of membrane processes in municipal wastewater reclamation and reuse. *Desalination, 178*(1-3), 1-11.

Wavefunction Inc., 18401 Von Karman Avenue, Suite 370, Irvine, CA 92612 U.S.A., www.wavefun.com.

Xiang, Y., Liu, Y., Mi, B., & Leng, Y. (2013). Hydrated polyamide membrane and its interaction with alginate: a molecular dynamics study. *Langmuir, 29*(37), 11600-11608.

Xiang, Y., Liu, Y., Mi, B., & Leng, Y. (2014). Molecular dynamics simulations of polyamide membrane, calcium alginate gel, and their interactions in aqueous solution. *Langmuir, 30*(30), 9098-9106.
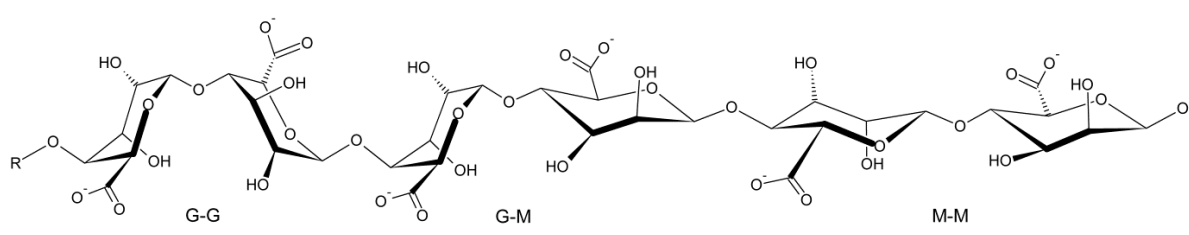
Fig. 1. A representative section of an alginate polymer chain displaying the two different monomers, G and M, and the three possible sequences. The carboxylate groups are deprotonated at a neutral pH.
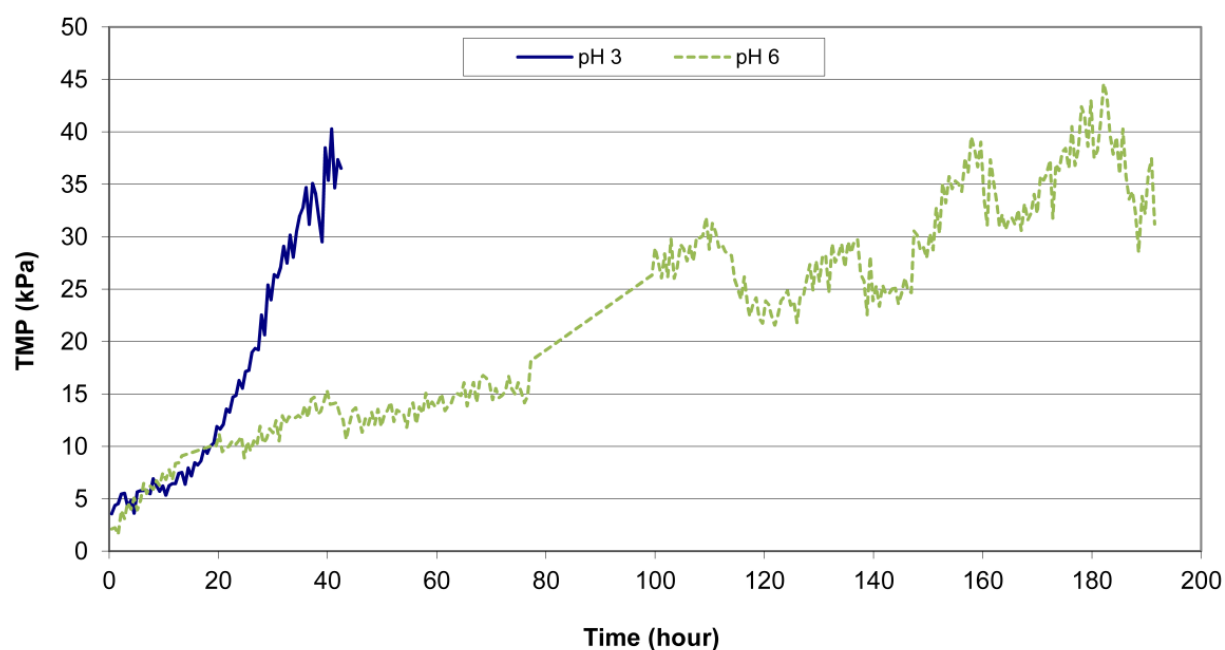

Fig. 2. Trans Membrane Pressure (TMP) versus time, comparing the fouling behaviour of sodium alginate under acidic (pH = 3 - solid blue line) and near neutral (pH = 6 - dotted green line) conditions, with respect to a hydrophobic polypropylene HF membrane.

(a)

(b)

(c)

(d)
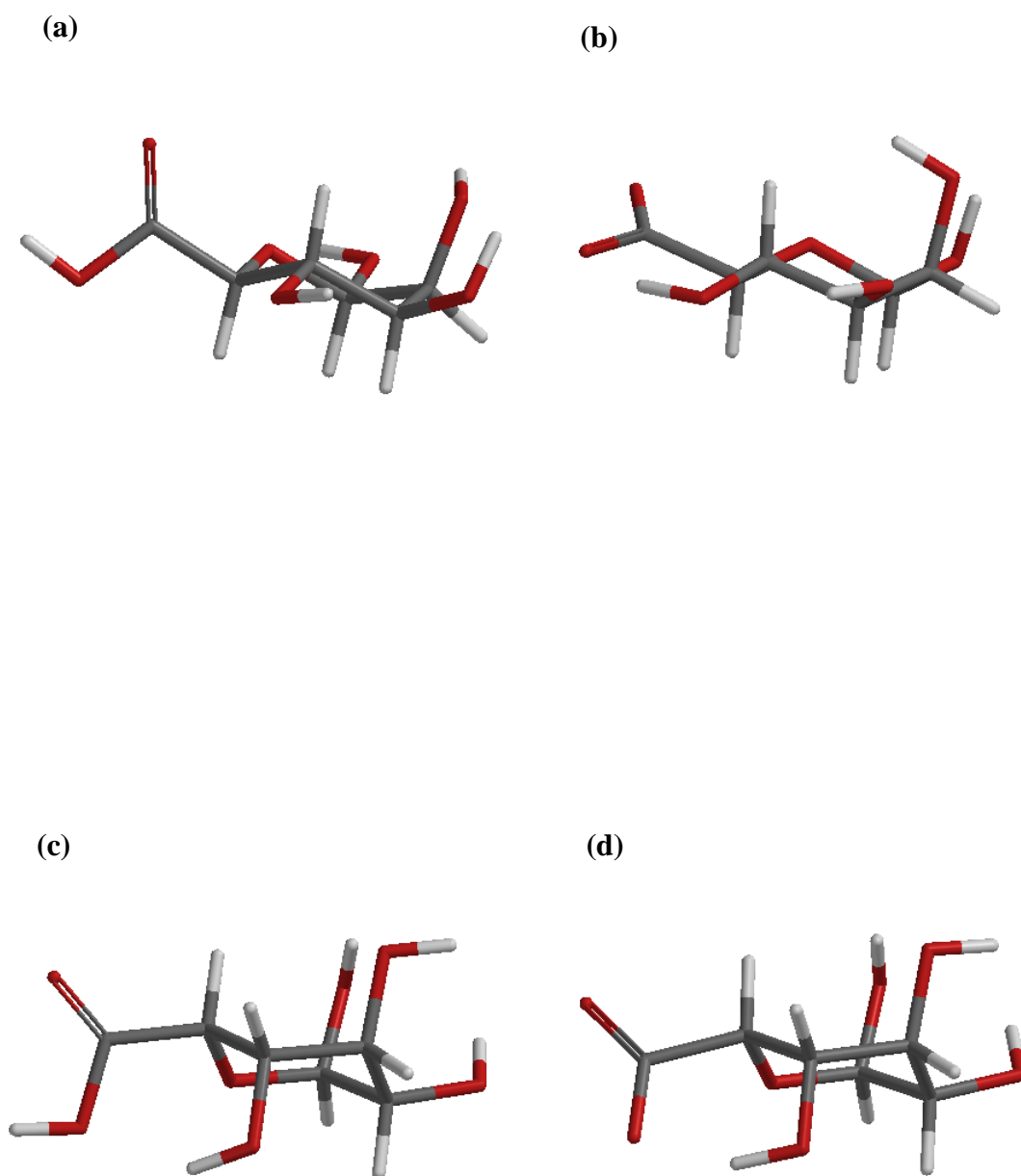
Fig. 3. Structural images of the calculated equilibrium geometries of the alginate monomers as viewed equatorially: **(a)** M protonated **(b)** M anionic **(c)** G protonated **(d)** G anionic. Of note is the isolation of the non-polar hydrogen atoms (white) on the underside of the M monomer in both the protonated and anionic structures, constituting a hydrophobic patch on one face. A similar motif is not present for the G monomers.

(a)

(b)

(c)

(d)
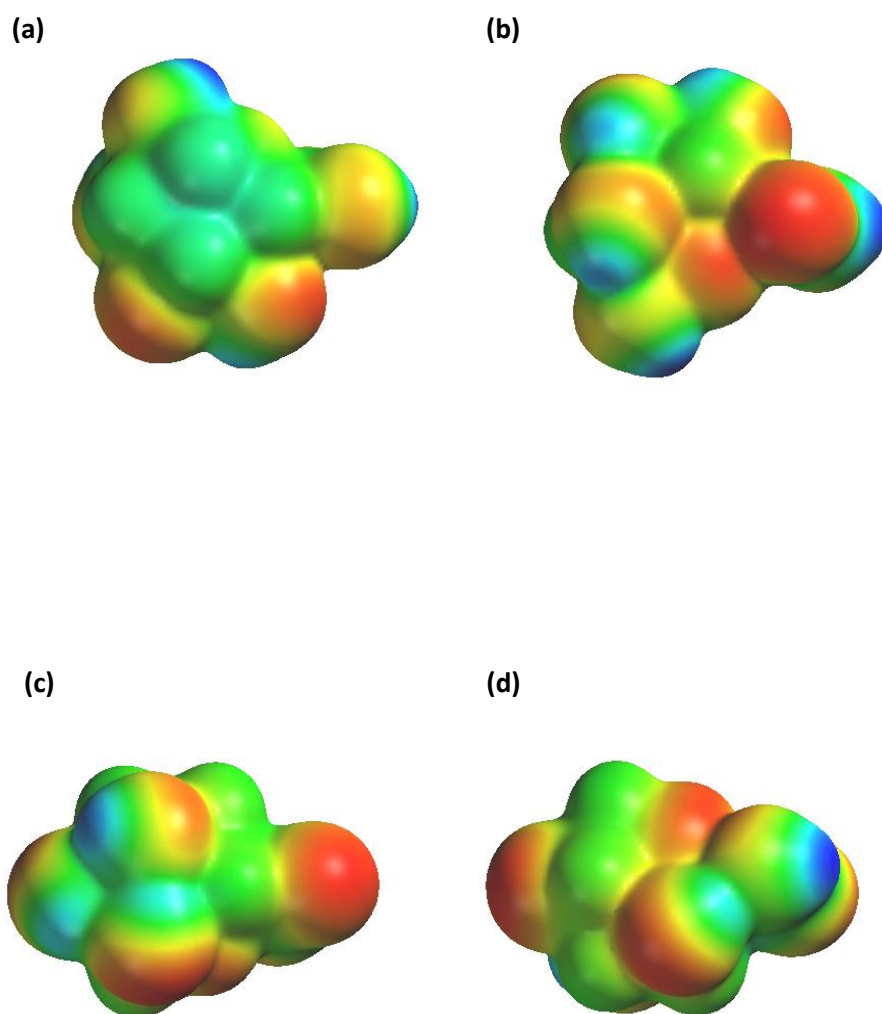
Fig. 4. Electrostatic potential energy maps (where red = negative electrostatic charge, blue = positive, green = neutral) of: **(a)** the charge-neutral face of the M monomer revealing the hydrophobic "patch" (green area); **(b)** the reverse side of the M monomer (180° rotation about the horizontal axis) showing the areas of positive (blue) and negative (red) electrostatic charge, hence hydrophilic; **(c)** one of the faces of the G monomer; **(d)** the other face of the G monomer (180° rotation about the horizontal axis) with both faces showing areas of positive (blue) and negative (red) electrostatic charge – hydrophilic.
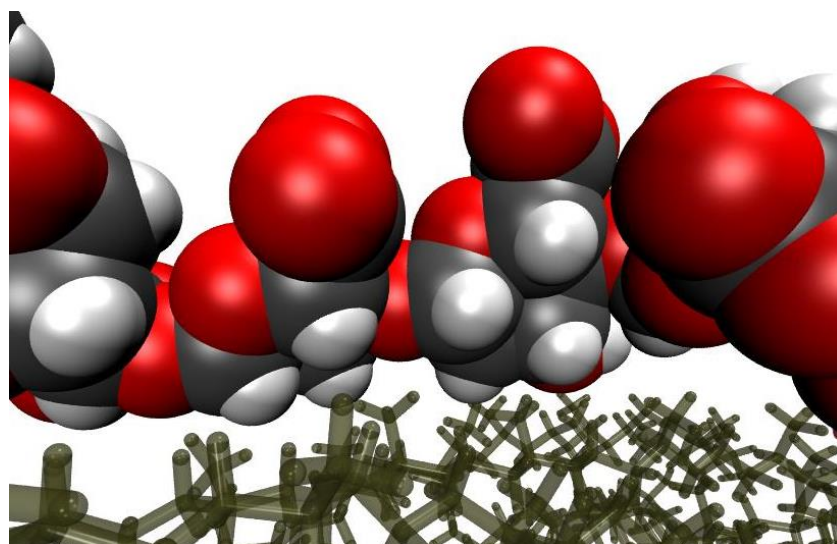
Fig. 5. The hydrophobic binding site identified on the GGMMGG hexamer (rendered as spheres), near the surface of the polypropylene model (rendered as transparent bonds). This binding site is formed by the two central M monomers of the hexamer, allowing both hydrophobic patches to access the surface simultaneously.
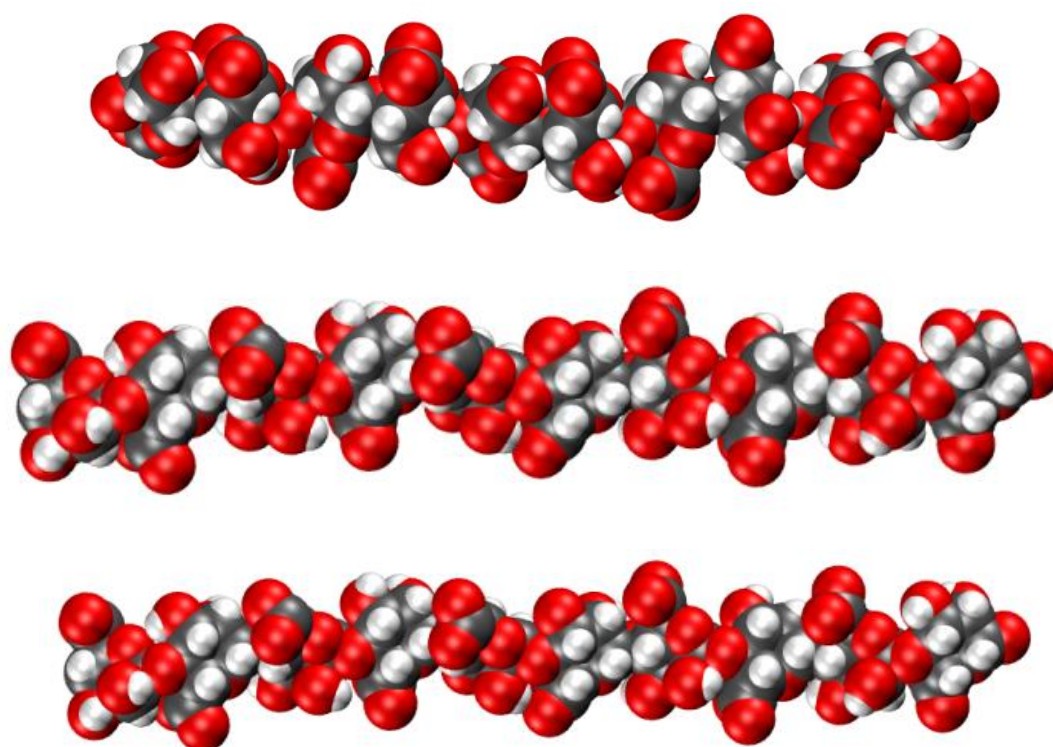
Fig. 6. Images of the three MD optimized decamer geometries – deca-G (top), deca-M (center) and penta-GM (lower) – from the perspective of the underside of the chains, showing a hydrophobic ribbon (deca-G) and hydrophobic patches (deca-M and penta-GM) as hightlighted by the white non-polar hydrogen atoms.

23
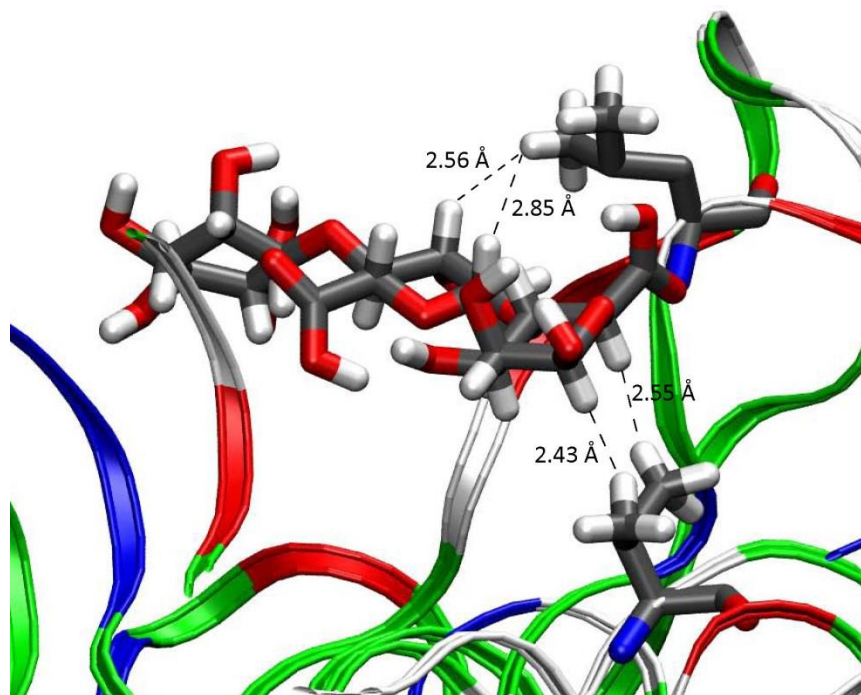
Fig. 7. Screenshot of the PDB-2PYH structure of mannuronan C-5 epimerase AlgE4, showing the interaction between the Leu-228 residue and the complexed tri-M ligand (top), and the interaction between the Val-201 residue with a hydrophobic patch on the complexed tri-M ligand (lower). Hydrogen positions have been estimated.

Table 1 The results of the low pH simulations, with the number of alginate chains interacting with the polypropylene surface and showing the *total* average interaction energy for the entire simulation.

Simulation	Number of chains contacting polypropylene surface		Total average van der Waals interaction energies (kcal/mol)
Deca-G-H	3		-81.289
Deca-M-H	7		-111.641
Penta-GM-H	9		-120.782